Planning Near-Optimal Corridors Amidst Obstacles*

Ron Wein[1], Jur van den Berg[2], and Dan Halperin[1]

[1] School of Computer Science, Tel-Aviv University
  {wein,danha}@tau.ac.il
[2] Institute of Information and Computing Sciences, Utrecht University
  berg@cs.uu.nl

Abstract. Planning corridors among obstacles has arisen as a central problem in game design. Instead of devising a one-dimensional motion path for a moving entity, it is possible to let it move in a corridor, where the exact motion path is determined by a local planner. In this paper we introduce a quantitative measure for the quality of such corridors. We analyze the structure of optimal corridors amidst point obstacles and polygonal obstacles in the plane, and propose an algorithm to compute approximations for optimal corridors according to our measure.

1 Introduction

The task of planning a natural path for a moving entity that avoids obstacles plays an important role in robotics, as well as in game design. The problem is often solved by constructing a graph that discretizes the environment, and extracting a collision-free path from this graph. The nodes of such a graph may be the cells of a uniform grid (see, e.g., [17]), or — according to Probabilistic Roadmap (PRM) paradigm [1, 5] — free configurations that are randomly chosen, attempting to capture the connectivity of the free configuration space.

A common drawback of the above methods is that they output a fixed path in response to a query. This is often not the ideal solution for motion planning, as it lacks flexibility to avoid local hazards (such as small obstacles, other moving entities, etc.) that are encountered during the motion. It also leads to predictable, and possibly unrealistic motions, which are not suitable for some applications, such as computer games. One approach for tackling these problems is a potential-field planner, in which the moving entity is attracted to its goal configuration, and repelled by obstacles, or other moving entities (see, e.g., [6]). However, this approach is prone to get stuck in local minima of the potential field; while there are methods that help in resolving such situations (see, e.g., [7]), they may still not yield valid motions at all.

We would therefore like to indicate the global direction of movement for the moving entity, while leaving enough flexibility for some *local planner* to avoid local hazards. An ideal solution for this is to use *corridors*, which have recently been introduced in the game design field [15]. Corridors are defined as a union of balls whose center points lie along a backbone path. The radius of the balls is determined by the *clearance* (i.e., the distance to the nearest obstacle) along the backbone path. The more restricted task of locally planning the motion around the backbone path can be successfully performed by potential-field methods. In order to guarantee that the local planner operates on a restricted environment, the radii of the balls are upper bounded by some predetermined value.[1] As a result, rather than moving along a fixed path, the moving entity moves within a corridor around the backbone path. This gives a strict global direction of movement, yet provides the local flexibility we look for.

Planning within corridors has many applications. It has been used to plan motions for coherent groups of entities, where the backbone path provides the global motion of the group [3]. The interactions between entities of the group are locally controlled by a social potential-field method [16]. Corridors have also been used to plan the motion of a camera that follows a moving character (a *guide*) [12]. If the guide moves along the backbone path, the corridor gives the flexibility for the camera to swerve if necessary. Another advantage of corridors is that they allow for non-holonomic and kinodynamic planning, if the motion of a single entity (or multiple entities) is planned using a potential field method within the corridor [4]. This is very difficult to achieve and incorporate into a fixed path. A common property of the applications of corridors is that the moving entity is small compared to the scale of the environment. In many fields (open field robotic navigation, games, etc.) this is indeed the case.

The problem we consider in this paper is how to plan a good corridor. A good corridor is short, avoiding unnecessary detours, and at the same time it should be wide (up to some prescribed maximum) to provide local maneuvering space. These requirements often contradict. Given start and goal configurations and a set of obstacles, the shortest collision-free path is contained in the *visibility graph* of the obstacles; see, e.g., [9]. However, such a path is incident to obstacle boundaries and cannot serve as a backbone path of a valid corridor. If one is only concerned with clearance, allowing paths that are as long as needed, then such paths are easily found using the *Voronoi diagram* of the given obstacles [14]. It is also possible to consider interpolates of these two structures, named *visibility–Voronoi diagrams*, as suggested in [19]. Indeed, a good corridor makes a good trade-off between length and clearance.

In this paper we introduce a measure for the quality of corridors, and present methods to plan corridors that are (nearly) optimal with respect to this measure amidst point obstacles or polygonal obstacles in the plane.

The rest of this paper is organized as follows. In Section 2 we formally define corridors and introduce the quality measure. Section 3 discusses properties of

---

[1] The fact that the radii of the balls are bounded is also a major difference between a corridor and the *medial axis transform* of the free workspace.

optimal corridors amidst point obstacles in the plane, and in Section 4 we generalize our results to polygonal obstacles. We give some concluding remarks and future-work directions in Section 5.

2   Measuring Corridors

A *corridor* $C = \langle \gamma(t), w(t), w_{\max} \rangle$ in a d-dimensional workspace (typically $d = 2$ or $d = 3$) is defined as the union of a set of d-dimensional balls whose center points lie along the *backbone path* of the corridor, which is given by the continuous function $\gamma : [0, L] \longrightarrow \mathbb{R}^d$, where L is the length of γ. The radii of the balls along the backbone path are given by the function $w : [0, L] \longrightarrow (0, w_{\max}]$. Both γ and w are parameterized by the length of the backbone path. In the following, we will refer to $w(t)$ as the *width* of the corridor at point t. The width is positive at any point along the corridor, and does not exceed $w_{\max}$, a prescribed *desired width* of the corridor.

Given a corridor $C = \langle \gamma(t), w(t), w_{\max} \rangle$ of length L in $\mathbb{R}^d$, the interior of the corridor is thus defined by $\bigcup_{t \in [0,L]} B\left(\gamma(t); w(t)\right)$, where $B(p; r)$ is an open d-dimensional ball with radius r that is centered at p. In typical motion-planning applications we are given a set of obstacles $\mathcal{O}$ that the moving entities should avoid. The interior of the corridor should be disjoint from the interior of the given obstacles, otherwise it is an *invalid* corridor. In this paper we study the problem of computing *valid* corridors amidst obstacles in the plane.

2.1   The Weighted Length Measure

As we have already indicated, a good corridor must be short — namely its backbone path should avoid unnecessarily long detours — and its width should be as wide as some predefined maximum in order to allow maximal flexibility for the motion within the corridor. The corridor should contain narrow passages only if they allow considerable shortcuts.

If we examine the intersection of the corridor $C = \langle \gamma(t), w(t), w_{\max} \rangle$ with an orthogonal $(d - 1)$-dimensional hyperplane at $\gamma(t)$, the volume of the cut is proportional to $w^{d-1}(t)$. Thus, in order to combine the two desired properties of the corridor as discussed above, we define the *weighted length* $L^*(C)$ of a corridor $C = \langle \gamma(t), w(t), w_{\max} \rangle$ to be:

$$L^*(C) = \int_{\gamma} \left(\frac{w_{\max}}{w(t)} \right)^{d-1} dt \ . \tag{1}$$

We wish to minimize the weighted length by either shortening the backbone path or by extending the corridor's width (up to $w_{\max}$). Given a start position $s \in \mathbb{R}^d$ and a goal position $g \in \mathbb{R}^d$, a corridor $C = \langle \gamma(t), w(t), w_{\max} \rangle$ satisfying $\gamma(0) = s$ and $\gamma(L) = g$ is *optimal* if for any other valid corridor C' connecting the two endpoints we have $L^*(C) \leq L^*(C')$.

Our weighting scheme can be directly applied for extracting backbone paths from PRMs that contain cycles [11, 13], where instead of considering the Euclidean length we try to minimize the weighted length of the backbone path we

compute, in order to obtain a better corridor. However, for some sets of obstacles we can actually devise a complete scheme for computing an optimal corridor, as we show in the rest of this paper.

2.2   Properties of an Optimal Corridor

Observation 1. *If for some portion of the backbone path γ of a corridor C, we have $w(t) < \min\{c(\gamma(t)), w_{\max}\}$ for $t \in [t_0, t_0 + \tau]$ ($\tau > 0$), where $c(p)$ is the* clearance *of the point p, namely its distance to the nearest obstacle, we can improve the quality of the corridor by letting $w(t) \longleftarrow \min\{c(\gamma(t)), w_{\max}\}$ for each $t \in [t_0, t_0 + \tau]$.*

Given a set of obstacles and a $w_{\max}$ value, we can associate the *bounded clearance* measure $\hat{c}(p)$ with each point $p \in \mathbb{R}^d$, where $\hat{c}(p) = \min\{c(p), w_{\max}\}$. Using the observation above, it is clear that the width function of an optimal path $C = \langle \gamma(t), w(t), w_{\max} \rangle$ is simply $w(t) = \hat{c}(\gamma(t))$. Note that $\hat{c}(\gamma(t))$ is a continuous function along any path γ.

Lemma 2. *Given a set of obstacles and $w_{\max}$, the backbone path of the optimal corridor connecting any given start position s with any goal position g is smooth.*

Proof. We have already observed that the weight function of the optimal corridor connecting s and g is the bounded clearance function of the backbone path and it is a continuous function. Assume that γ contains a sharp turn (a $\mathcal{C}_1$-discontinuity). Let us shortcut the sharp turn using a circular arc of radius r (as r approaches 0 the approximation is tighter). Let ℓ_1 be the length of the original path segment we shortcut and let ℓ_2 be the length of the circular arc. It is easy to show that there exist $\hat{r} > 0$ and some constants $A_1 > A_2 > 0$ such that for each $0 < r < \hat{r}$ we have $\ell_1 \geq A_1 r$ and $\ell_2 = A_2 r$. If the maximal width w^* along the original path segment is obtained at some point p^*, then as the distance of any point p along the circular arc from p^* is bounded by Kr, where K is some constant, and as the weight function is continuous, we can write $w^* - w(p) < Mr$ for some positive constant M. Let L_1^* be the weighted length of the original path segment and let L_2^* be the weighted length of the circular arc. We can write:

$$\frac{L_1^*}{L_2^*} \geq \frac{\frac{w_{\max}}{w^*} l_1}{\frac{w_{\max}}{w^* - Mr} l_2} = \frac{w^* - Mr}{w^*} \cdot \frac{A_1}{A_2} \ .$$

As $A_1 > A_2$, we can choose $0 < r < \min\left\{\frac{w^*}{M}\left(1 - \frac{A_2}{A_1}\right), \hat{r}\right\}$ such that the entire expression above is greater than 1. We thus have $L_1^* > L_2^*$, and we managed to decrease the weighted length of the corridor, in contradiction to its optimality. We conclude that $\gamma(t)$ must be a smooth function.   □

At several places in this paper we apply infinitesimal analysis, where we assume that the bounded clearance measure (hence the weight function) is not continuous. Assume that we have some hyperplane $\mathcal{H}$ in $\mathbb{R}^d$ that separates two regions, such that in one region the bounded clearance is w_1 and in the other it is w_2.

Minimizing the weighted length between two endpoints that are separated by $\mathcal{H}$ is equivalent to applying Fermat's principle, stating that the actual path between two points taken by a beam of light is the one which is traversed in the least time. The optimal backbone thus crosses the separating hyperplane once, such that the angles α_1 and α_2 it forms with the normal to $\mathcal{H}$ obey Snell's Law of refraction,[2] with w_1 and w_2 playing the role of the "speed of light" in the respective regions:

$$w_2 \sin \alpha_1 = w_1 \sin \alpha_2 \ . \tag{2}$$

3 Optimal Corridors Amidst Point Obstacles

In this section we consider planar environments cluttered with point obstacles $p_1, \ldots, p_n \in \mathbb{R}^2$ and a preferred corridor width $w_{\max}$. Given two endpoints $s, g \in \mathbb{R}^2$, we show how to compute a (near-)optimal corridor that connects s and g.

3.1 A Single Point Obstacle

Let us assume we have a single point obstacle p. Without loss of generality we assume p is located at the origin. We start with computing an optimal corridor between two endpoints whose distance from p is smaller than or equal to $w_{\max}$. Note that the width of such a corridor at $\gamma(t)$ along its backbone is $\|\gamma(t)\|$.

We first approximate the optimal backbone by a polyline: for any $\Delta r > 0$, if we look at the circles of radii $\Delta r, 2\Delta r, 3\Delta r, \ldots$ that are centered at the origin, each two neighboring circles define an annulus; since Δr is small we assume that the distance from p of all points in the kth annulus is constant and equals $k\Delta r$. Consider the scenario depicted in Figure 1(a), where γ enters one of the annuli at some point A, where $\|A\| = r_1$, and leaves this annulus at B, where $\|B\| = r_2 = r_1 + \Delta r$. The angles that the backbone path forms with pA and pB are α_1 and β_1, respectively. When entering the annulus we have $w_1 = r_1$ and $w_2 = r_2$, so applying Equation (2) we can express the refracted angle α_2, using $\sin \alpha_2 = \frac{r_2}{r_1} \sin \alpha_1$. By applying the Law of Sines on the triangle $\triangle pAB$, we get $\frac{r_2}{\sin(\pi - \alpha_2)} = \frac{r_1}{\sin \beta_1}$, therefore:

$$\sin \beta_1 = \frac{r_1}{r_2} \sin(\pi - \alpha_2) = \frac{r_1}{r_2} \sin \alpha_2 = \sin \alpha_1 \ .$$

Thus $\beta_1 = \alpha_1$. Taking $\Delta r \longrightarrow 0$, we obtain a smooth curve γ, such that the angle that $\nabla\gamma(t)$ forms with $\overrightarrow{p\gamma(t)}$ is a constant ψ. It is possible to show that a curve that has this property must be segment of a *logarithmic spiral* (also named an *equiangular spiral*)[3] whose polar equation is given by $r(t) = ae^{b\theta(t)}$, where a is a constant and $b = \cot \psi$. See, e.g., [2] for a proof of this latter fact.

---

[2] See, e.g., `http://scienceworld.wolfram.com/physics/SnellsLaw.html` for the details and for a detailed proof. See also Mitchell and Papadimitriou [10], who used this observation in a similar setting of the problem.
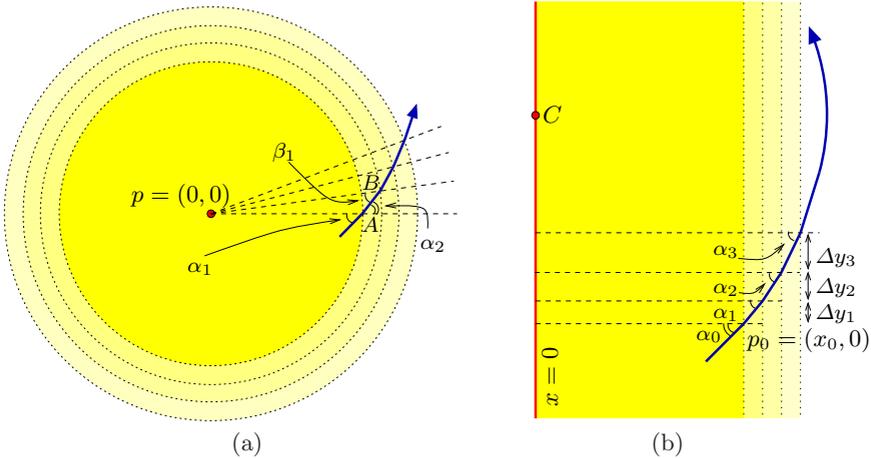
[3] `http://www-groups.dcs.st-and.ac.uk/~history/Curves/Equiangular.html`

Fig. 1. Analysis of the optimal backbone path in the vicinity of a single obstacle: (a) near a point obstacle $p = (0,0)$, (b) near a line segment supported by $x = 0$

Proposition 3. *Given a single point obstacle located at the origin, a start position $s = r_s e^{i\theta_s}$ and a goal position $g = r_g e^{i\theta_g}$ (in polar coordinates), where $r_s, r_g \leq w_{max}$, the backbone of the optimal corridor connecting s and g is a spiral arc supported by the logarithmic spiral $r = a^* e^{b^* \theta}$. Since both s and g lie on this spiral, we have (assuming $\theta_s \neq \theta_g$, otherwise the optimal backbone path is simply a line segment):*

$$a^* = r_g^{\frac{\theta_s}{\theta_s - \theta_g}} \cdot r_s^{-\frac{\theta_g}{\theta_s - \theta_g}} \ , \qquad b^* = \frac{1}{\theta_g - \theta_s} \cdot \ln \frac{r_g}{r_s} \ . \qquad (3)$$

We now consider the case where the clearance of the two endpoints exceeds w_{max}, namely the two endpoints of our path lie outside the closure of the disc $B(p; w_{max})$. There are two possible scenarios: (i) The straight line segment $\overline{sg}$ does not intersect $B(p; w_{max})$; in this case, this segment is the backbone of the optimal corridor. (ii) $\overline{sg}$ intersects $B(p; w_{max})$. In this latter case the optimal backbone path is a bit more involved. Consider some backbone path γ connecting s and g. It is clear that the intersection of γ with $B(p; w_{max})$

comprises a single component, so we denote the point where the path enters the disc by s' and the point where it leaves the disc by g' (see the illustration to the right). As s' and g' lie on the disc boundary, their polar representation is $s' = w_{max} e^{i\theta_{s'}}$ and $g' = w_{max} e^{i\theta_{g'}}$, so we use Equation (3) and obtain $a^* = w_{max}$ and $b^* = 0$. The optimal path between s' and g' therefore lies on the degenerate spiral $r = w_{max}$, namely the circle that forms the boundary of $B(p; w_{max})$. We conclude that the
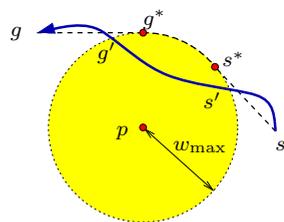
optimal backbone path between s and g must contain a circular arc on the boundary of $B(p; w_{\max})$. As according to Lemma 2 this path must be smooth, it should comprise two line segments ss^* and g^*g that are tangent to the disc and a circular arc that connects the two tangency points s^* and g^* (see the dashed path in the figure above). Note that as there are two possible smooth paths from s to g we select the shortest one.

3.2 Multiple Well-Separated Point Obstacles

Let us now go back to our original setting, where we are given a set of point obstacles $\mathcal{O} = \{p_1, \ldots, p_n\}$, along with a preferred width $w_{\max}$, and wish to compute the optimal corridor from s to g, where we assume that $c(s) = \min_i \|s - p_i\| \geq w_{\max}$ and $c(g) = \min_i \|g - p_i\| \geq w_{\max}$.

In case the points are well separated — that is, for each $i \neq j$ the discs $B(p_i; w_{\max})$ and $B(p_j; w_{\max})$ are disjoint in their interiors (implying that $\|p_i - p_j\| \geq 2w_{\max}$), we can follow the same arguments we used above for a single obstacle and conclude that the optimal backbone is either the straight line segment sg (in case it is *free*, namely its interior does not intersect the interior of any of the discs), or it comprises circular arcs and line segments that connect them.

We can therefore construct the visibility graph of the dilated obstacles and use it to construct optimal paths. The vertices of this graph are the endpoints of the free bitangents to two dilated obstacles, which in turn are represented as graph edges. In addition, each two neighboring tangency points on a disc $B(p_i; w_{\max})$ are connected by a circular arc. Given a path-planning query, namely two endpoints s and g, we treat s and g as vertices and add all free tangents from s and from g to the discs as graph edges. If the segment sg is free, we add it to the graph as well. We then perform Dijkstra's algorithm from s to find the shortest path to g in the resulting graph. The weight $\omega(e)$ given to each graph edge e is its weighted length, which simply equals its length in this case.

Proposition 4. *Given a set $\mathcal{O}$ of n point obstacles in the plane that are well-separated with respect to $w_{\max}$, and two endpoints s and g with clearance at least $w_{\max}$, it is possible to compute the optimal corridor connecting s and g in $O(E \log n)$ time using the visibility graph of the dilated obstacles, where E is the number of visibility edges in this graph.*

3.3 Corridors Amidst Point Obstacles: The General Case

We now consider the case where the endpoints s and g have arbitrary clearance, namely the dilated obstacles $B(p_1; w_{\max}), \ldots, B(p_n; w_{\max})$ are not necessarily pairwise disjoint in their interiors. The boundary of $\mathcal{M} = \bigcup_{i=1}^n B(p_i; w_{\max})$ comprises whole circles and circular arcs, such that a common endpoint of two arcs is a reflex vertex. We now construct $\mathcal{V}$, the Voronoi diagram of the points, and compute the intersection $\mathcal{V} \cap \mathcal{M}$, namely the portions of the Voronoi edges contained within the union of the dilated obstacles. Note that reflex vertices are equidistant to two point obstacles, so they serve as the connection points between

the Voronoi edges and the boundary arcs
of $\mathcal{M}$. We will refer to the Voronoi edges
in $\mathcal{V} \cap \mathcal{M}$, together with the circular arcs
that form the boundary of $\mathcal{M}$, as the
bounded Voronoi diagram of the point set
$\mathcal{O} = \{p_1, \ldots, p_n\}$, which we denote $\hat{\mathcal{V}}(\mathcal{O})$.
The figure to the right shows the bounded
Voronoi diagram of six points; the bound-
ary of $\mathcal{M}$ is drawn is solid lines and the
Voronoi edges are dotted.
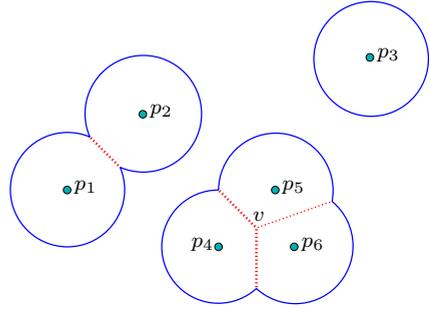
Note that $\hat{\mathcal{V}}(\mathcal{O})$ partitions the plane
into two-dimensional cells of two types: Voronoi regions of the point obstacles,
and regions where the clearance is larger than $w_{\max}$. Given two points s' and g'
that belong to the same cell κ, we know that:

- If κ is a cell whose clearance is greater than $w_{\max}$, the optimal backbone
  path between $s' = (x_1, y_1)$ and $g' = (x_2, y_2)$ is the straight line segment σ
  that connects them, provided that σ does not intersect any feature of $\hat{\mathcal{V}}(\mathcal{O})$.
  The weighted length of this segment simply equals the Euclidean distance
  $\|g' - s'\| = \sqrt{(x_2 - x_1)^2 + (y_2 - y_1)^2}$.
- If κ is a Voronoi cell of a point obstacle p_i, the optimal backbone path between
  s' and g' is a spiral arc σ centered at p_i, provided that σ does not intersect
  any feature of $\hat{\mathcal{V}}(\mathcal{O})$. If $s' = r_1 e^{i\theta_1}$ and $g' = r_2 e^{i\theta_2}$ are the polar coordinates of
  the endpoints with respect to p_i, the weighted length of σ is given by (recall
  that from Equation (3) we have $b = \frac{1}{\theta_2 - \theta_1} \cdot \ln \frac{r_2}{r_1}$):

$$L^*(\sigma) = \int_{\theta_1}^{\theta_2} \frac{w_{\max}}{r(\theta)} \sqrt{r^2(\theta) + \left(\frac{dr}{d\theta}\right)^2 (\theta)} \, d\theta = \int_{\theta_1}^{\theta_2} \frac{w_{\max}}{ae^{b\theta}} \sqrt{1 + b^2} ae^{b\theta} \, d\theta =$$

$$= \int_{\theta_1}^{\theta_2} w_{\max} \sqrt{1 + b^2} \, d\theta = w_{\max} \sqrt{1 + b^2} (\theta_2 - \theta_1) =$$

$$= w_{\max} \sqrt{(\theta_2 - \theta_1)^2 + (\ln r_2 - \ln r_1)^2} \ .$$

In addition, the features of $\hat{\mathcal{V}}(\mathcal{O})$ are also *locally optimal*, namely they can serve
as backbone paths of optimal corridors (see Figure 2(a)). We already know that
portions of the circular arcs that form the boundary of $\mathcal{M}$ are locally optimal,
and that the weighted length of such a circular arc simply equals its length.
The Voronoi edges are also locally optimal: given s' and g' on the same Voronoi
edge, the optimal backbone path that connects them is simply the straight line
segment $s'g'$ which coincides with the Voronoi edge.

Following the construction of the visibility graph of the dilated point obstacles
(Section 3.2), it is possible to add *visibility edges* to the bounded Voronoi dia-
gram, namely to consider every free bitangent of two circular arcs, every free line
segment from a reflex vertex tangent to a circular arc and every free line segment
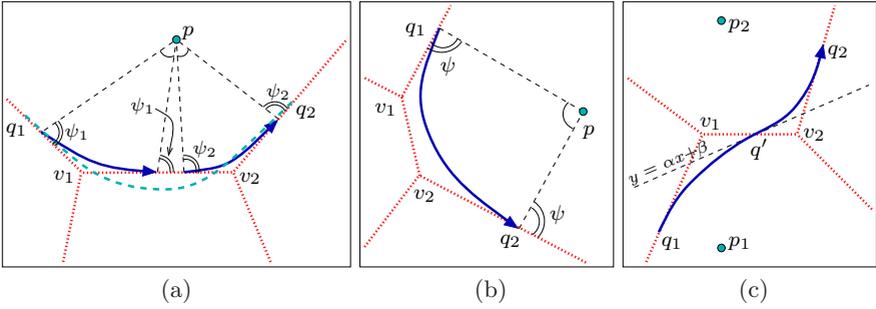
Fig. 2. (a) The spiral arc connecting q_1 and q_2 (dashed) crosses the Voronoi edge v_1v_2; the optimal backbone path between q_1 and q_2 therefore comprises two spiral arcs that shortcut v_1 and v_2 (solid arrows) and portions of Voronoi edges. (b) Shortcutting two adjacent Voronoi vertices v_1 and v_2 by a single spiral arc. (c) Shortcutting two Voronoi vertices by a cross-cell curve, which is a smooth concatenation of two spiral arcs. Both arcs have a common tangent $y = \alpha x + b$, which crosses the Voronoi edge v_1v_2 at q'.

between two reflex vertices.[4] However, a path extracted from such a graph may pass through Voronoi vertices and reflex vertices, thus it may contain sharp turns. According to Lemma 2, such a path cannot serve as a backbone to an optimal corridor. We can try and rectify this problem by introducing a *shortcut edge* between each pair of Voronoi edges that are incident to a common Voronoi vertex (see Figure 2(a) for an illustration), and between each pair consisting of a Voronoi edge and a visibility edge that are both incident to a common reflex vertex. However, this is not sufficient. We can show that it is sometimes possible to shortcut two Voronoi vertices v_1 and v_2 at once by connecting two Voronoi edges that are separated by another edge using a single curve. This curve may be contained in a single Voronoi cell, as in the example depicted in Figure 2(b), or it may cross the Voronoi edge v_1v_2 at some point q' (see Figure 2(c)). We should continue and examine the possibility of shortcutting $k > 2$ Voronoi vertices by considering sequences of $(k + 1)$ contiguous Voronoi edges and trying to locate an endpoint q_1 on the first edge and q_2 on the last edge that are connected by a smooth curve comprising spiral arcs. This operation is not trivial, and requires solving a system of low-degree polynomial equations with $2(N_c + 1)$ unknowns, where N_c is the number of crossings between the shortcut curve and the Voronoi diagram. In some scenarios it may be possible to construct shortcuts to $\Theta(n)$ Voronoi vertices by considering sequences of $\Theta(n)$ contiguous Voronoi edges, thus the size of the augmented diagram may blow up exponentially.

We therefore devise an approximation algorithm based on the structure of the bounded Voronoi diagram $\hat{\mathcal{V}}(\mathcal{O})$ and the planar partition it induces. Given $\varepsilon > 0$, we subdivide the line segments and the circular arcs that form the features of

---

[4] The resulting construct is the visibility–Voronoi diagram of the obstacles; see [19] for more details.

$\hat{\mathcal{V}}(\mathcal{O})$ into small intervals of length $\frac{c(I)}{w_{\max}}\varepsilon$ (as ε is small, we consider the clearance of an interval I to be constant and denote it $c(I)$). Notice that the intervals are shorter in regions where the clearance is smaller, and that each interval has weighted length ε. Hence, if Λ is the total weighted length of the features of $\hat{\mathcal{V}}(\mathcal{O})$, then there are $\frac{\Lambda}{\varepsilon}$ intervals in total. Let us now define a graph $\mathcal{D}$ whose set of nodes equals the set of intervals $\mathcal{I}$. Each interval is incident to two of the cells defined by the bounded Voronoi diagram, and we connect $I_1, I_2 \in \mathcal{I}$ by an edge if and only if they are incident to a common cell. This edge is a line segment in a cell where the clearance is larger than $w_{\max}$, a spiral segment in a Voronoi region of one of the point obstacles, a circular arc on the boundary of a dilated obstacle, or a straight line segment on a Voronoi edge. In addition, an edge should not cross any of the features of $\hat{\mathcal{V}}(\mathcal{O})$. Using a brute-force algorithm that checks each candidate edge versus the $O(n)$ diagram features, $\mathcal{D}$ can be constructed in $O\left(\frac{\Lambda^2}{\varepsilon^2}n\right)$ time.

Given two endpoints s and g, we can connect them to the graph and use Dijkstra's algorithm to compute a near-optimal backbone connecting s and g in $O\left(\frac{\Lambda^2}{\varepsilon^2}\right)$ time. Let γ^* be the backbone path of the optimal corridor between s and g, which comprises $k = O(n)$ segments $\gamma_1, \ldots, \gamma_k$ (a path segment may be a straight line segment, a spiral arc, a portion of a circular arc or a portion of a Voronoi edge). We next show that each such segment is approximated by an edge in the graph $\mathcal{D}$ we have constructed.

Lemma 5. *For each segment γ_i of the optimal backbone path γ^*, there exists an edge e in $\mathcal{D}$ such that $L^*(e) < L^*(\gamma_i) + 2\sqrt{2}\varepsilon$.*

Proof. Let us denote the endpoints of the path segment γ_i by q_1 and q_2, and let I_1 and I_2 be the intervals that contain these endpoints, respectively.

In case γ_i is a straight line segment in a cell κ whose clearance is greater than $w_{\max}$, then its weighted length simply equals $\|q_2 - q_1\|$, the Euclidean distance between its endpoints. In the graph $\mathcal{D}$ there exists an edge connecting I_1 and I_2, and we denote its endpoints by $\tilde{q}_1$ and $\tilde{q}_2$. By the construction of the intervals, we know that $\|q_j - \tilde{q}_j\| \leq \frac{c(I_j)}{w_{\max}}\varepsilon = \varepsilon$ (for $j = 1, 2$), hence:

$$\|\tilde{q}_2 - \tilde{q}_1\| < \|q_2 - q_1\| + 2\varepsilon \ .$$

Similar arguments hold when γ_i is a circular arc with clearance $w_{\max}$.

In case γ_i is a segment on a Voronoi edge, the graph $\mathcal{D}$ contains a segment $\tilde{q}_1\tilde{q}_2$ that in the worst case extends $\frac{c(q_1)}{w_{\max}}\varepsilon$ to one side of q_1 and $\frac{c(q_2)}{w_{\max}}\varepsilon$ to the other side of q_2. Since the contribution of each of these extensions is $\frac{w_{\max}}{c(q_j)}$ times its length (for $j = 1, 2$), the weighted length of $\tilde{q}_1\tilde{q}_2$ is at most 2ε more than $L^*(\gamma_i)$.

The case where γ_i is a spiral arc contained in a Voronoi cell of a point obstacle p_i is a bit more involved. Let $q_1 = r_1 e^{i\theta_1}$ and $q_2 = r_2 e^{i\theta_2}$ be the polar coordinates of γ_i's endpoints with respect to p_i, then we have $L^*(\gamma_i) = w_{\max}\sqrt{(\theta_2 - \theta_1)^2 + (\ln r_2 - \ln r_1)^2}$. $\mathcal{D}$ contains a spiral arc connecting I_1 and I_2, and we denote its endpoints by $\tilde{q}_j = \tilde{r}_j e^{i\tilde{\theta}_j} \in I_j$ (for $j = 1, 2$). As $c(q_j) = r_j$,

we know that the length of each of these two intervals is $\|I_j\| = \frac{r_j}{w_{\max}}\varepsilon$. If we denote $\Delta\theta_j = \theta_j - \tilde{\theta}_j$, we can write:

$$\sin\left(\frac{\Delta\theta_j}{2}\right) < \frac{\frac{1}{2}\|I_j\|}{r_j} = \frac{\varepsilon}{2w_{\max}} \ .$$

As for small angles $\sin\phi \approx \phi$, we conclude that $|\Delta\theta_j| < \frac{\varepsilon}{w_{\max}}$. At the same time, $|\Delta r_j| = |r_j - \tilde{r}_j| < \frac{\varepsilon r_j}{w_{\max}}$, thus we have:

$$|\ln \tilde{r}_j - \ln r_j| < \left|\ln\left(r_j\left(1 + \frac{\varepsilon}{w_{\max}}\right)\right) - \ln r_j\right| = \ln\left(1 + \frac{\varepsilon}{w_{\max}}\right) \ .$$

As $\ln(1+x) \approx x$ for small x values, we conclude that $|\ln \tilde{r}_j - \ln r_j| < \frac{\varepsilon}{w_{\max}}$. The length of the approximated spiral arc contained in $\mathcal{D}$ can therefore be at most $L^*(\gamma_i) + 2\sqrt{2}\varepsilon$. $\qquad\square$

Corollary 6. *For each two endpoints s and g, it is possible to use the graph $\mathcal{D}$ and compute a near-optimal backbone path $\tilde{\gamma}$ connecting s and g in $O\left(\frac{\Lambda^2}{\varepsilon^2}\right)$ time, such that $L^*(\tilde{\gamma}) < L^*(\gamma^*) + O(n)\varepsilon$.*

4   Optimal Corridors Amidst Polygonal Obstacles

In this section we generalize the data structures introduced in Section 3 to compute optimal corridors amidst polygonal obstacles. As we did in case of point obstacles, we first examine how an optimal backbone path looks like in the vicinity of a single obstacle. Note that the polygon P can be viewed as a collection of points (vertices) and line segments (edges), such that the distance of a point $q \in \mathbb{R}^2$ to P is attained on a polygon vertex or in the interior of an edge. We can thus subdivide the plane into regions, such that the identity of the closest polygon feature is the same for all points in any of the regions. Using the analysis we performed in Section 3.1 we already know that the optimal backbone path in a region closest to a polygon vertex is an arc of a logarithmic spiral. We now study the case of two points that lie in a region closest to a polygon edge.

Without loss of generality, we shall assume that the polygon edge we consider is an arbitrarily long segment of the vertical line $x = 0$, and analyze the optimal backbone path γ between two points s and g, whose distance from this line is less than $w_{\max}$ (see Figure 1(b) for an illustration). Note that the width of the corridor at $\gamma(t) = (x(t), y(t))$ simply equals $|x(t)|$.

We begin by approximating the backbone path by a polyline. Assume that $\gamma(t)$ passes through a point $p_0 = (x_0, 0)$ and forms an angle α_0 with the line $y = 0$ perpendicular to the obstacle. For any $\Delta x > 0$ we can define the lines $x = x_0, x = x_0 + \Delta x, x = x_0 + 2\Delta x, \ldots$, where each two neighboring lines define a vertical slab; since Δx is small we assume that the distance of all points in the slab from

the obstacle is constant and equals $x_0 + k\Delta x$. We can now use Equation (2) and write: $\sin \alpha_1 = \frac{x_0+\Delta x}{x_0} \sin \alpha_0$, $\sin \alpha_2 = \frac{x_0+2\Delta x}{x_0+\Delta x} \sin \alpha_1 = \frac{x_0+2\Delta x}{x_0} \sin \alpha_0$, ..., $\sin \alpha_k = \frac{x_0+k\Delta x}{x_0} \sin \alpha_0$. If we examine the kth slab we can write $x = x_0 + k\Delta x$, so we have:

$$\Delta y_k = \Delta x \tan \alpha_k = \Delta x \cdot \frac{\sin \alpha_k}{\sqrt{1 - \sin^2 \alpha_k}} = \Delta x \cdot \frac{x \sin \alpha_0}{\sqrt{x_0^2 - x^2 \sin^2 \alpha_0}} . \quad (4)$$

Letting Δx tend to zero we obtain a smooth curve. We can use Equation (4) to express the derivative of the curve and we obtain:

$$y'(x) = \lim_{\Delta x \longrightarrow 0} \frac{\Delta y_k}{\Delta x} = \frac{x \sin \alpha_0}{\sqrt{x_0^2 - x^2 \sin^2 \alpha_0}} , \quad (5)$$

$$y(x) = -\frac{1}{\sin \alpha_0} \sqrt{x_0^2 - x^2 \sin^2 \alpha_0} + K . \quad (6)$$

As the point $(x_0, 0)$ lies on the curve, it is easy to see that the constant K equals $x_0 \cot \alpha_0$.

Observe that $y(x)$ is defined only for $x < \frac{x_0}{\sin \alpha_0}$. When $x = \frac{x_0}{\sin \alpha_0}$ the path is reflected from the vertical wall and starts approaching the obstacle. We note that squaring and re-arranging Equation (6) we obtain that $x^2 + (y - x_0 \cot \alpha_0)^2 = \left(\frac{x_0}{\sin \alpha_0}\right)^2$, thus we conclude that γ is a circular arc, whose supporting circle is centered at $C = (0, x_0 \cot \alpha_0)$ and its radius is $\frac{x_0}{\sin \alpha_0}$.

Proposition 7. *Given a start position $s = (x_s, y_s)$ and a goal position $g = (x_g, y_g)$ in the vicinity of a segment supported by $x = 0$ and with $0 < x_s, x_g \le w_{\max}$, the backbone of the optimal corridor between these two endpoints is a circular arc supported by a circle of radius r^* that is centered at $(0, y^*)$, where (we assume that $y_s \ne y_g$, otherwise the optimal backbone path is simply the line segment sg):*

$$y^* = \frac{y_s + y_g}{2} + \frac{x_g^2 - x_s^2}{2(y_g - y_s)} , \quad (7)$$

$$r^* = \sqrt{\frac{1}{2}(x_s^2 + x_g^2) + \frac{1}{4}(y_g - y_s)^2 + \frac{(x_g^2 - x_s^2)^2}{4(y_g - y_s)^2}} . \quad (8)$$

4.1   Moving Amidst Multiple Polygons

We are given a set $\mathcal{P} = \{P_1, \ldots, P_k\}$ of polygonal obstacles having n vertices in total, along with a preferred corridor width $w_{\max}$.

We first mention that if the polygons are well-separated, namely the distance between each P_i and P_j ($1 \le i < j \le k$) is more than $2w_{\max}$, we can use the visibility graph of the dilated polygons to plan optimal backbone paths. The dilated obstacles in this case are Minkowski sums of the polygonal obstacles with a disc of radius $w_{\max}$ and their boundary comprises line segments, which correspond to dilated polygon edges, and circular arcs, which correspond to

dilated vertices. Visibility edges in this case correspond to line segments tangent to two circular arcs. Proving that the visibility graph indeed contains optimal backbone paths is done exactly the same as we did in Section 3.2 for point obstacles.

In case there exist narrow passages between the obstacles, we generalize the construction detailed in Section 3.3 to polygons, and introduce the bounded Voronoi diagram of the set of polygons $\mathcal{P}$. Note that in this case we have *Voronoi chains* that are sequences of Voronoi edges. A Voronoi edge may be induced by two polygon vertices or by two polygon edges, in which case it is a line segment, or by a polygon vertex and an edge of another polygon, in which case it is a parabolic arc. Thus, the Voronoi chains are smooth curves that are piecewise linear or piecewise parabolic and are equidistant to two nearest polygons; see, e.g., [8] for more details. The bounded Voronoi diagram $\hat{\mathcal{V}}(\mathcal{P})$ also contains edges that separate the Voronoi cells of adjacent polygon features, namely a polygon edge and a vertex incident to this edge. These edges are line segments perpendicular to the obstacles (see Figure 3 for an illustration).

Observe that if we are given two points on the same Voronoi chain, then the locally optimal backbone path between them is simply the segment of the chain they define. This is clear in case of point obstacles, as the edges are straight line segments. In case of chains that separate Voronoi cells of polygons and may contain parabolic arcs this fact is less obvious. However, we are able to prove that parabolic arcs are also locally optimal — namely, it is not possible to shortcut such an arc by choosing a shorter route that is closer to one of the polygons, as such a route always has a larger weighted length. This proof is rather technical and we refer the reader to [18] for its details.

$\hat{\mathcal{V}}(\mathcal{P})$ subdivides the plane into cells of three types: regions where the clearance is larger than $w_{\max}$, Voronoi cells of polygon vertices, and Voronoi cells of polygon edges. We have already encountered cells of the first two types in the bounded Voronoi diagram of a set of points (Section 3.3). We also know from Proposition 7 that if we have two points in the Voronoi cell of a polygon edge, the optimal backbone path connecting them is a circular arc whose center lies on this edge. Assume, without loss of generality, that the obstacle edge lies on the line $y = 0$ and that the center of the circular arc a is the origin, and let $r^* e^{i\theta_1}$ and $r^* e^{i\theta_2}$ be the arc endpoints. The weighted length of the circular arc is therefore given by (note that $r(\theta) = r^*$):

$$L^*(a) = \int_{\theta_1}^{\theta_2} \frac{w_{\max}}{r^* \sin\theta} \sqrt{r^2(\theta) + \left(\frac{dr}{d\theta}\right)^2(\theta)} \, d\theta = \int_{\theta_1}^{\theta_2} \frac{w_{\max}}{\sin\theta} \, d\theta =$$

$$= w_{\max} \left(\ln \frac{1 - \cos\theta}{\sin\theta} \right) \Big|_{\theta_1}^{\theta_2} = w_{\max} \left(\ln \tan \frac{\theta_2}{2} - \ln \tan \frac{\theta_1}{2} \right) .$$

The approximation algorithm given in Section 3.3 can also be extended to handle polygonal obstacles. In this case we also consider intervals that lie on Voronoi edges that separate the Voronoi cell of each polygon into simple regions — thus, each region is induced by a polygon vertex, a polygon edge, or correspond to regions where the clearance is above $w_{\max}$. We can show that Lemma 5 also
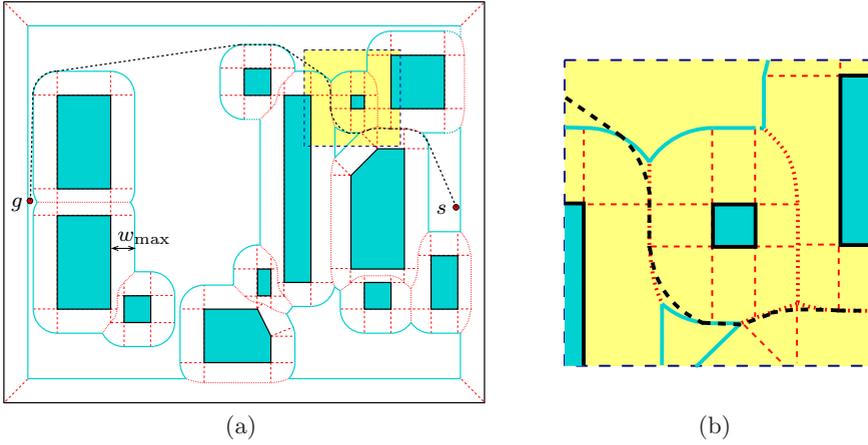
$$(a) \qquad\qquad\qquad\qquad (b)$$

Fig. 3. (a) A near-optimal backbone path (dashed) amidst polygonal obstacles, over-layed on top of the the bounded Voronoi diagram of the obstacles. Boundary edges are drawn in light solid lines, Voronoi chains between polygons are dotted, and Voronoi edges that separate cells of adjacent polygon features are drawn in a light dashed line. The bounded Voronoi diagram was computed using the software described in [19]. The backbone path was computed using an A* algorithm on a fine grid discretizing the environment. (b) Zooming on a portion of the path; notice the shortcuts that the path takes.

applies for the circular arcs inside a Voronoi cell of a polygon edge: Let γ_i be such a circular arc and let I_1 and I_2 be the intervals containing its endpoints q_1 and q_2, receptively. $\mathcal{D}$ contains a circular arc σ connecting I_1 and I_2, and we denote its endpoints $\tilde{q}_j = \tilde{r}_j e^{i\tilde{\theta}_j} \in I_j$ (for $j = 1, 2$). As $c(q_j) = r^* \sin\theta_j$, we know that the length of each interval is $\|I_j\| = \frac{r^* \sin\theta_j}{w_{\max}}\varepsilon$. If we denote $\Delta\theta_j = \theta_j - \tilde{\theta}_j$, we can write:

$$\sin\left(\frac{\Delta\theta_j}{2}\right) < \frac{\frac{1}{2}\|I_j\|}{r^*} = \frac{\varepsilon}{2w_{\max}}\sin\theta_j \ .$$

As for small angles $\sin\phi \approx \phi$, we conclude that $|\Delta\theta_j| < \frac{\varepsilon}{w_{\max}}\sin\theta$. If we use the fact that $f(x + \Delta x) \approx f(x) + f'(x)\Delta x$ (for small Δx) with $f(x) = \ln\tan\frac{x}{2}$, we can bound the weighted length of σ (recall that $f'(x) = \frac{1}{\sin x}$ in our case):

$$L^*(\sigma) = w_{\max}\left(\ln\tan\frac{\theta_2 + \Delta\theta_2}{2} - \ln\tan\frac{\theta_1 + \Delta\theta_1}{2}\right) <$$

$$w_{\max}\left(\ln\tan\frac{\theta_2}{2} + \frac{\varepsilon\sin\theta_2}{w_{\max}}\cdot\frac{1}{\sin\theta_2} - \ln\tan\frac{\theta_1}{2} + \frac{\varepsilon\sin\theta_1}{w_{\max}}\cdot\frac{1}{\sin\theta_1}\right) = L^*(\gamma_i) + 2\varepsilon \ .$$

Corollary 8. *Given a set of polygonal obstacles $\mathcal{P}$ having n vertices in total, let Λ be the total weighted length of the bounded Voronoi diagram $\hat{\mathcal{V}}(\mathcal{P})$ with*

respect to a given $w_{\max}$ value. Given $\varepsilon > 0$, we can construct a graph $\mathcal{D}$ over the intervals of $\hat{\mathcal{V}}(\mathcal{P})$ in $O\left(\frac{\Lambda^2}{\varepsilon^2}n\right)$ time, such that for each two endpoints s and g it is possible to use $\mathcal{D}$ and compute a near-optimal backbone of a corridor C connecting s and g. $L^*(C)$ is at most $O(n)\varepsilon$ more than the weighted length of the optimal corridor connecting s and g.

5 Conclusions and Future Work

In this paper we have introduced a measure for the quality of corridors and studied the structure of optimal corridors amidst point obstacles and polygonal obstacles in the plane. We have devised an approximation algorithm for computing near-optimal corridors amidst obstacles. We are also investigating methods to speed up our approximation algorithm, as well as design simple practical methods to compute good corridors. We are interested in extending our result to corridors in three dimensions as well.

In some applications having a winding backbone path decreases the quality of the corridor. We can therefore augment the weighted length function by considering the curvature of the backbone path γ as follows:

$$L^*_\mu(C) = \int_\gamma \left(\frac{w_{\max}}{w(t)}\right)^{d-1} dt + \mu \int_\gamma w(t)\kappa(t)dt \ , \tag{9}$$

where $\kappa(t)$ is the curvature of $\gamma(t)$, and $0 < \mu \leq 1$ is the weight we give to the curvature measure. We are able to show that in case of well-separated obstacles, optimal corridors under the L^*_μ measure are still contained in the visibility graph of the obstacles dilated by $w_{\max}$. We are still exploring methods of computing optimal corridors in the case of denser scenes.

References

1. Choset, H., Lynch, K.M., Hutchinson, S., Kantor, G., Burgard, W., Kavraki, L.E., Thrun, S.: Principles of Robot Motion: Theory, Algorithms, and Implementations, ch.7. MIT Press, Boston (2005)
2. Gray, A.: Modern Differential Geometry of Curves and Surfaces with Mathematica. In: Logarithmic Spirals, 2nd edn., pp. 40–42. CRC Press, Boca Raton (1997)
3. Kamphuis, A., Overmars, M.H.: Motion planning for coherent groups of entities. In: Proc. IEEE Int. Conf. Robotics and Automation, pp. 3815–3822 (2004)
4. Kamphuis, A., Pettre, J., Overmars, M.H., Laumond, J.-P.: Path finding for the animation of walking characters. In: Proc. Eurographics/ACM SIGGRAPH Sympos. Computer Animation, pp. 8–9 (2005)
5. Kavraki, L.E., Švestka, P., Latombe, J.-C., Overmars, M.H.: Probabilistic roadmaps for path planning in high-dimensional configuration spaces. IEEE Trans. Robotics and Automation 12, 566–580 (1996)
6. Khatib, O.: Real-time obstacle avoidance for manipulators and mobile robots. Int. J. Robotics Research 5(1), 90–98 (1986)

7. Latombe, J.-C.: Robot Motion Planning, ch. 7. Kluwer Academic Publishers, Boston (1991)
8. Lee, D.-T., Drysdale III, R.L.: Generalization of Voronoi diagrams in the plane. SIAM J. on Computing 10(1), 73–87 (1981)
9. Mitchell, J.S.B.: Shortest paths and networks. In: Goodman, J.E., O'Rourke, J. (eds.) Handbook of Discrete and Computational Geometry, ch.27, 2nd edn., pp. 607–642. Chapman & Hall/CRC, Boca Raton (2004)
10. Mitchell, J.S.B., Papadimitriou, C.H.: The weighted region problem: Finding shortest paths through a weighted planar subdivision. J. of the ACM 38(1), 18–73 (1991)
11. Nieuwenhuisen, D., Kamphuis, A., Mooijekind, M., Overmars, M.H.: Automatic construction of roadmaps for path planning in games. In: Proc. Int. Conf. Computer Games: Artif. Intell., Design and Education, pp. 285–292 (2004)
12. Nieuwenhuisen, D., Overmars, M.H.: Motion planning for camera movements. In: Proc. IEEE Int. Conf. Robotics and Automation, pp. 3870–3876 (2004)
13. Nieuwenhuisen, D., Overmars, M.H.: Useful cycles in probabilistic roadmap graphs. In: Proc. IEEE Int. Conf. Robotics and Automation, pp. 446–452 (2004)
14. Ó'Dúnlaing, C., Yap, C.K.: A "retraction" method for planning the motion of a disk. J. Algorithms 6, 104–111 (1985)
15. Overmars, M.H.: Path planning for games. In: Proc. 3rd Int. Game Design and Technology Workshop, pp. 29–33 (2005)
16. Reif, J., Wang, H.: Social potential fields: a distributed behavioral control for autonomous robots. In: Goldberg, K., Halperin, D., Latombe, J.-C., Wilson, R. (eds.) International Workshop on Algorithmic Foundations of Robotics, pp. 431–459. A. K. Peters (1995)
17. Russel, S., Norvig, P.: Artificial Intelligence: A Modern Approach, 2nd edn. Prentice Hall, Englewood Cliffs (2002)
18. Wein, R., van den Berg, J., Halperin, D.: Planning near-optimal corridors amidst obstacles. Technical report, Tel-Aviv University (2006),
http://www.cs.tau.ac.il/~wein/publications/pdfs/corridors.pdf
19. Wein, R., van den Berg, J.P., Halperin, D.: The visibility-Voronoi complex and its applications. In: Proc. 21st Annu. ACM Sympos. Comput. Geom., pp. 63–72 (2005); In: Computational Geometry: Theory and Applications (to appear)